frontiers | Frontiers in Energy Research

BRIEF RESEARCH REPORT
published: 11 July 2022
doi: 10.3389/fenrg.2022.967167

Optimal Reconfiguration of Thermoelectric Generation System Under Heterogeneous Temperature Difference

You Zheng[1], *Enyou Zhang*[2] *and Peng An*[1]*

[1]School of Electronic and Information Engineering, Ningbo University of Technology, Ningbo, China, [2]Ningbo Jianan Electronics Company Limited., Ningbo, China

In view of the low efficiency of thermoelectric generation systems in different regions, this paper designs an optimization and reconfiguration of thermoelectric power generation system under heterogeneous temperature difference (HTD) based on particle swarm optimization (PSO) algorithm, so as to make full use of various thermal energy resources and obtain higher electrical output power, which realize multi-directional utilization of energy. In addition, PSO algorithm is a simple optimization strategy with a straightforward operation mechanism and fewer parameters to control during calculation. The research shows that when TEG array is in multiple HTD states, PSO algorithm has a stronger ability to get rid of local optimization, which can reduce power loss and improve energy conversion efficiency. On this basis, PSO algorithm is used to reconfigure the 15 × 15 symmetric TEG array. The experimental simulation analysis based on MATLAB platform is carried out to verify the feasibility of PSO algorithm.

Keywords: thermoelectric generation system, heterogeneous temperature difference, reconfiguration, particle swarm optimization algorithm, symmetric

OPEN ACCESS

Edited by:
Xueqian Fu,
China Agricultural University, China

Reviewed by:
Yaxing Ren,
University of Warwick, United Kingdom
Yixuan Chen,
University of Hong Kong, Hong Kong SAR, China

***Correspondence:**
Peng An
614545513@qq.com

Specialty section:
This article was submitted to Smart Grids, a section of the journal Frontiers in Energy Research

Received: *12 June 2022*
Accepted: *22 June 2022*
Published: *11 July 2022*

Citation:
Zheng Y, Zhang E and An P (2022) Optimal Reconfiguration of Thermoelectric Generation System Under Heterogeneous Temperature Difference. Front. Energy Res. 10:967167. doi: 10.3389/fenrg.2022.967167

1 INTRODUCTION

With the growth of the global population and the improvement of human living standards (Shahbaz et al., 2020; Sun et al., 2020), energy consumption is also growing rapidly. For more than 100 years, traditional fossil energy (Liu et al., 2020) has been dominant in energy consumption, even disasters to a certain extent (Yang et al., 2020), but the consumption of traditional fossil energy will generate a large amount of carbon dioxide, which will lead to obvious greenhouse gas effects and bring huge challenges (Zhang et al., 2019) to the living environment of human beings, even to a certain degree of disaster. Thus, based on new materials and new technologies, the development of clean and renewable energy that can replace traditional fossil energy (El-Dein et al., 2013) (i.e., hydropower, nuclear energy, solar energy, wind energy, hydrogen energy, etc.) is imminent, which plays a vital role in the optimization of energy structure as well as the protection of the ecological environment.

It is worth noting that modern human activities generate a large amount of waste heat (Jian et al., 2021), especially industrial production activities are the main reason for creating a large amount of waste heat. Based on this, many scholars currently use semiconductor thermoelectric generation (Ge et al., 2021) technology to convert this waste heat into electricity. Thermoelectric generator (TEG) (Fernández-Yáñez et al., 2021), also known as waste heat power generation, is based on the theory of thermoelectric power generation, that is, using the temperature difference between high and low temperature heat

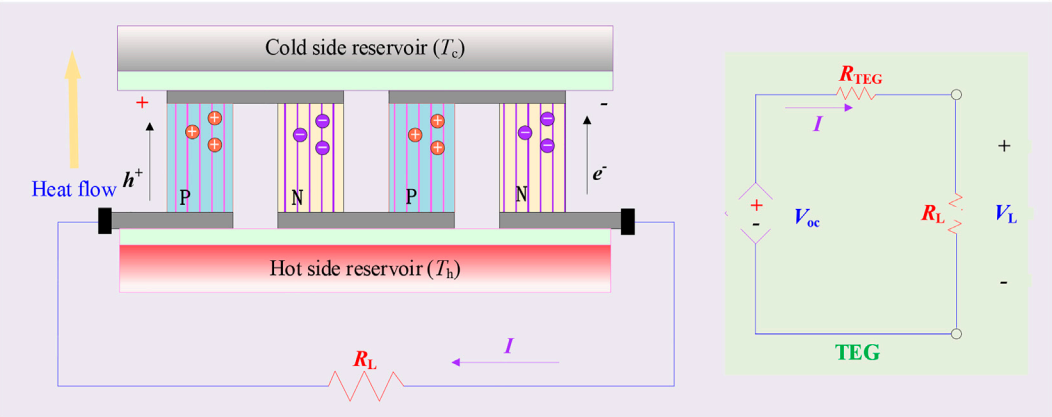

FIGURE 1 | Equivalent circuit of a TEG module.

sources, upon which low boiling point working fluid is used as the circulating work fluid. And then, on the basis of Rankine Cycle (RC), the steam generated by the high temperature heat source is heated and evaporated to generate electricity, which can directly convert the heat source into electricity, while the power generation process is vibration-free, pollution-free, highly reliable, long service life, etc. In addition, TEG system (Luo et al., 2021) has numerous application scenarios, such as temperature differences between upper and lower ocean waters, waste heat from automobile engines, and waste heat generated from industrial equipment after the operation.

Although TEG has tremendous potential in the field of waste heat recovery, its inherent deficiencies such as low energy conversion efficiency and low waste heat utilization rate restrict its more extensive application. One of the ideas being researched to enhance energy conversion efficiency is to search for the maximum power point (MPP) based on the maximum power point tracking (MPPT) algorithm. For the TEG array in uniform temperature difference conditions (i.e., similar to photovoltaic (PV) (Li et al., 2018) panels exposed to various solar radiation), scholars have concentrated a large number of their attention. Traditional gradient control techniques (Mamura et al., 2022) such as perturbation observation (PO) method, incremental conductance (INC.) method, open circuit voltage (OCV) method, and other optimization methods are exploited to obtain the optimal energy output of the TEG system. Although the traditional methods mentioned above are straightforward (Matthew and Jae, 2015) in principle and easy to implement, they are less accurate in control, which oscillates significantly around the MPP and even misjudges it, thus causing some power loss. Besides, in practical engineering applications, the external ambient temperature is not constant, rather it changes dynamically, which renders the gradient control techniques unsuitable for MPPT under various heterogeneous temperature difference (HTD) conditions.

The inevitable actual HTD states can produce multiple local maximum power points (LMPPs) on the power curve, into which the above method can be trapped very easily, so more sophisticated and intelligent techniques are required to search for the global maximum power point (GMPP). The meta-heuristic algorithms are powerful tools for achieving high-quality solutions in a short time, in part by identifying locally optimal solutions in the absence of an exact mathematical model. They offer an insightful and promising direction of work for tackling complicated high-dimensional optimization problems. Reference (Yang et al., 2019) proposed an improved adaptive compass search (ACS) to realize an efficient and stable GMPP search on power-current (*P-I*) of centralized TEG system under HTD. The proposed arithmetic optimization algorithm (AOA) in literature (Zhang et al., 2022), based on arithmetic operators in mathematics, enabled simple and rapid adaptive local exploration and global exploitation, thereby avoiding low quality LMPP to raise the energy utilization efficiency and generation efficiency of TEG systems. In addition, the musical chairs algorithm (MCA), particle swarm optimization (PSO) (Lamzouri et al., 2020), cuckoo search algorithm (CSA), as well as genetic algorithm (GA) are also applied to the MPPT of TEG systems.

With further research into energy efficiency and generation efficiency improvements in TEG systems, inspired by PV array reconfiguration for maximum power output, reconfiguration of TEG arrays is also a promising approach. In special, the reconfiguration technology can be divided into static reconfiguration and dynamic reconfiguration. The former reduces the power loss by rearranging the physical location of the PV modules. Although this method can disperse the shadows to other rows, the wiring is not flexible and inefficient for large PV arrays. Therefore, in practical engineering applications, dynamic reconfiguration has greater potential, which is to dynamically change the electrical connection mode by changing the switch matrix with strong flexibility and reliability. It is worth affirming that meta-heuristic algorithms have significant advantages and potential in dealing with array reconfiguration. For instance, butterfly optimization algorithm (BOA) (Fathy, 2020), grasshopper optimization algorithm (GOA) (Fathy, 2018), gravitational search algorithm (GSA) (Hasanien et al., 2016) artificial ecosystem-based optimization (AEO) (Yousri et al., 2022), ant colony algorithm (ACO) (Krishnan et al., 2020), and so on.

Inspired by the reconfiguration of PV arrays, this paper proposes a novelist PSO algorithm (Zeddini et al., 2016) for

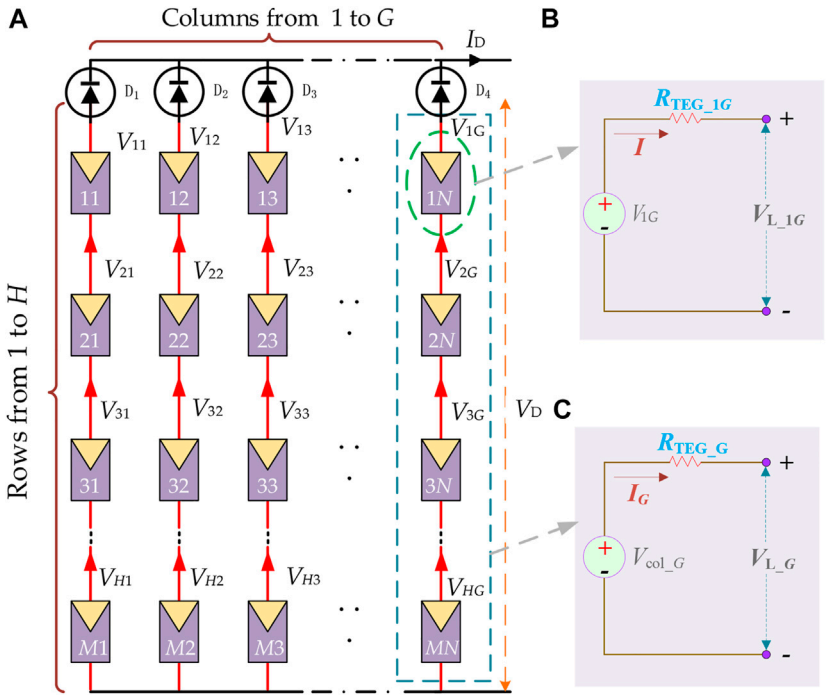

FIGURE 2 | The $M \times N$ topology of the TEG array. **(A)** shows the H × G topology of the TEG array. **(B)** plots the circuit equivalent of a single TEG module. **(C)** gives the equivalence circuit diagram for the Nth column TEG array.

the reconfiguration of TEG arrays to reduce power losses and boost power generation efficiency. The main novelties/contributions of the proposed method are stated as follows:

- The concept of reconfiguring TEG array to maximize power output is proposed for the first time;
- PSO algorithm is a simple group optimization strategy with a simple operation mechanism and few parameters to be controlled in the calculation process;
- The experimental results illustrate that PSO algorithm has a stronger ability to get rid of falling into local optimization, which can reduce power loss and improve energy conversion efficiency when TEG array is in multiple HTD states.

The rest of this paper is presented as follows: the mathematical model of TEG array is provided in **Section 2**. Besides, **Section 3** describes the execution mechanism of PSO algorithm in detail. **Section 4** illustrates results and discussion of simulation in comprehensive cases. Lastly, **Section 5** summarizes various conclusions and future perspectives.

2 TEG ARRAY MODELLING

2.1 TEG Module Modelling

The TEG module is composed of two different thermoelectric materials, i.e., p-type and n-type. In addition, based on the Seebeck effect principle, the potential difference is caused by the migration of carriers in thermoelectric materials to convert heat energy into electric energy, as presented in **Figure 1**. A TEG module can be equivalent to a series resistance of the current source, which can be written as follows (Liu et al., 2016):

$$V_{oc} = \alpha_{pn}(T_h - T_c) = \alpha_{pn}\Delta T \tag{1}$$

where α_{pn} means the Seebeck coefficient (μV/K); T_h and T_c denote the temperature on the hot side and cold side, respectively (℃); ΔT is the temperature difference (℃).

The Seebeck coefficient α_{pn} is normally a temperature function that depends mainly on the conductor which is positively correlated with temperature. Additionally, the Thompson effect also plays a role in the generation of heat, with the Thomson coefficient τ being written as (Liu et al., 2016; Bijukumar et al., 2018)

$$\tau = T\frac{d\alpha_{pn}}{dT} \tag{2}$$

where T is the average temperature of the hot side and cold side.

In practice, the Seebeck coefficient varies dynamically, mainly according to the average temperature on the low temperature side as well as on the high temperature side, which can be indicated as (Chakraborty et al., 2006)

$$\alpha(T) = \alpha_0 + \alpha_1 \ln(T/T_0) \tag{3}$$

where α_0 denotes the fundamental portion of Seebeck coefficient; α_1 stands for the variation rate of Seebeck coefficient; T_0 is regarded as the temperature reference.

TABLE 1 | Executive procedure of PSO algorithm based on reconfiguration.

1	Input six HTD conditions
2	Initialize the parameters and population
3	Set k: = 0
4	Calculate the objective function value $f(k)$ of all the searching individuals by **Eq. 15**
5	WHILE $k < k_{max}$
6	For i = 1,2, … , N
7	Update the velocity of particles by **Eq. 17**
8	Check particle velocity boundaries
9	Update the position of particles by **Eq. 18**
10	Check particle position boundaries
11	Update the objective function value $f(k)$ again by **Eq. 15**
12	IF $f(X_i) < f(Pbest_i)$ then
13	$Pbest_i = X_i$
14	$f(Pbest_i) = f(X_i)$
15	END
16	IF $f(Pbest) < f(Gbest_i)$ then
17	$Gbest_i = Pbest_i$
18	$f(Gbest_i) = f(Pbest_i)$
19	Set k: = k+1
20	END WHILE
21	Output the optimal solution and the best fitness

Figure 1 represents the equivalent circuit of the TEG module, where the output current I_{TEG} as well as the output power P_{TEG} of the TEG module can be derived as

$$I_{\mathrm{TEG}} = \frac{V_{\mathrm{oc}}}{R_{\mathrm{L}} + R_{\mathrm{TEG}}} \tag{4}$$

$$P_{\mathrm{TEG}} = \left(\alpha_{\mathrm{pn}}\Delta T\right)^2 \frac{\mathrm{R_L}}{\left(R_{\mathrm{L}} + R_{\mathrm{TEG}}\right)^2} \tag{5}$$

where P_{TEG} is the output power of TEG module; R_{TEG} is the internal resistance; R_{L} presents load resistance.

When the external load is equivalent to the internal resistance of the thermoelectric material, the maximum power value can be obtained in the thermoelectric circuit as follows:

$$P_{\max} = \frac{V_{\mathrm{oc}}^2}{4 \cdot R_{\mathrm{TEG}}} \tag{6}$$

2.2 Mathematical Modelling of TEG Array

The low output voltage and low power of a single TEG module make it difficult to satisfy the practical requirements of the application, so several modules are connected in parallel and in series to form a TEG array. **Figure 2A** shows the $H \times G$ topology of the TEG array. **Figure 2B** plots the circuit equivalent of a single TEG module. **Figure 2C** gives the equivalence circuit diagram for the Nth column TEG array.

The output voltage and corresponding internal resistance in each column of the TEG array can be written as the sum of the voltages and corresponding internal resistances of the TEG modules in that column, which represents as

$$V_{\mathrm{col\_}g} = \sum_{h=1}^{H} V_{hg} \quad h = 1, 2, 3, \ldots, H; g = 1, 2, 3, \ldots, G \tag{7}$$

$$R_{\mathrm{TEG\_}g} = \sum_{h=1}^{H} R_{\mathrm{TEG\_}hg} \tag{8}$$

where V_{hg} is the voltage from the hth row and the gth column; $R_{\mathrm{TEG\_}g}$ presents the overall resistance in the nth column; $R_{\mathrm{TEG\_}hg}$ is denoted as the corresponding internal resistance of the hth row and the gth column.

There is no doubt that the output power of a TEG array is highly dependent on the load voltage. Because when the output voltage of the column is less than the load voltage, the column is considered to be resistive. On the contrary, this column can output power. The equivalent internal resistance of each TEG module is calculated as

$$R_{\mathrm{e\_TEG}_g} = \begin{cases} R_{\mathrm{TEG\_}g} & \text{if } V_n \geq V_{\mathrm{L}} \\ \infty & \text{others} \end{cases} \tag{9}$$

Furthermore, each column of TEG array can be equated to a current source in parallel with the corresponding internal resistance, whereas the current source can be expressed as

$$I_{\mathrm{col\_}g} = \frac{V_{\mathrm{col\_}g}}{R_{\mathrm{e\_TEG}_g}} \tag{10}$$

The equivalent circuit of the $H \times G$ topology TEG array can be simplified to G current sources in parallel. Besides, the current sources in the circuit can be equated to voltage sources according to Thevenin's theorem. Consequently, the total internal resistance, current sources, and voltage source of the TEG array can be written as follows:

$$R_{\mathrm{s\_TEG}} = \frac{1}{\sum_{h=1}^{H} \frac{1}{R_{\mathrm{e\_TEG}_h}}} \tag{11}$$

$$I_{\mathrm{s\_TEG}} = \sum_{h=1}^{H} I_{\mathrm{col\_}h} \tag{12}$$

$$V_{\mathrm{s\_TEG}} = R_{\mathrm{s\_TEG}} \cdot I_{\mathrm{s\_TEG}} \tag{13}$$

The TEG array can output the maximum power when the total internal resistance is equal to the load resistance. Hence, the maximum output power of the TEG array can be described as

$$P_{\mathrm{s\_max}} = \frac{V_L^2}{4 \cdot R_{\mathrm{s\_TEG}}} = \frac{\left(\frac{1}{2} \cdot V_{\mathrm{s\_TEG}}\right)^2}{4 \cdot R_{\mathrm{s\_TEG}}} = \frac{V_{\mathrm{s\_TEG}}^2}{16 \cdot R_{\mathrm{s\_TEG}}} \tag{14}$$

2.3 Objective Function

The significance of TEG array reconfiguration lies in seeking for GMPP, whose mathematical formula can be constructed as

$$f(k) = P_{\mathrm{s\_max}} = \max\left(\sum_{h=1}^{H} I_l \times V_l\right) = \frac{\mathrm{V}_{\mathrm{s\_TEG}}^2}{16 \cdot R_{\mathrm{s\_TEG}}} \tag{15}$$

2.4 Power Enhancement

Furthermore, a key criterion to measure the efficiency and performance of reconfiguration is power enhancement, which can be expressed as

$$P_{\mathrm{en}} = \frac{G_{\mathrm{mpp_{re}}} - G_{\mathrm{mpp_{no}}}}{G_{\mathrm{mpp_{no}}}} \times 100\% \tag{16}$$

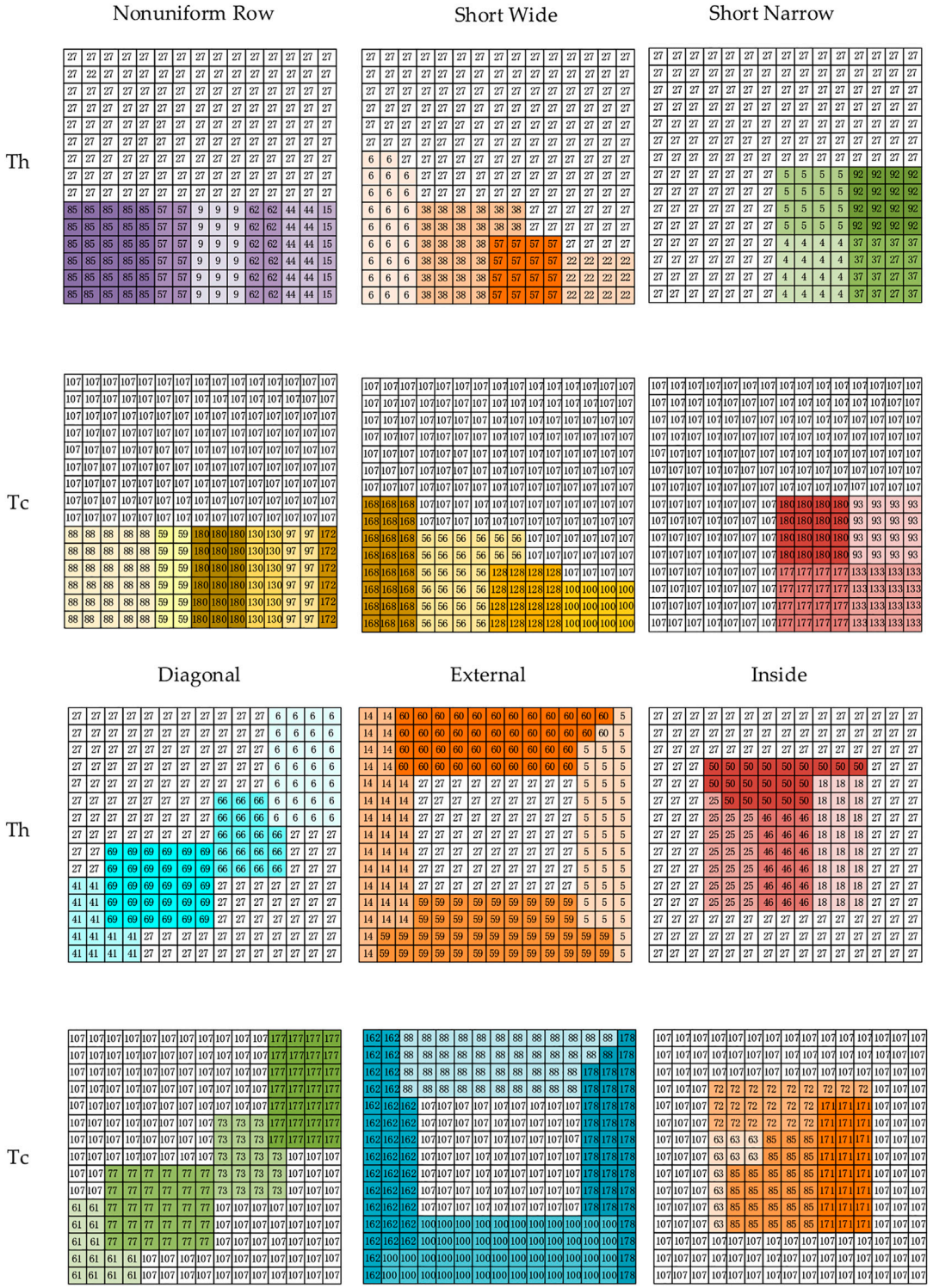

FIGURE 3 | Six HTD patterns in the 15 × 15 symmetric TEG array.

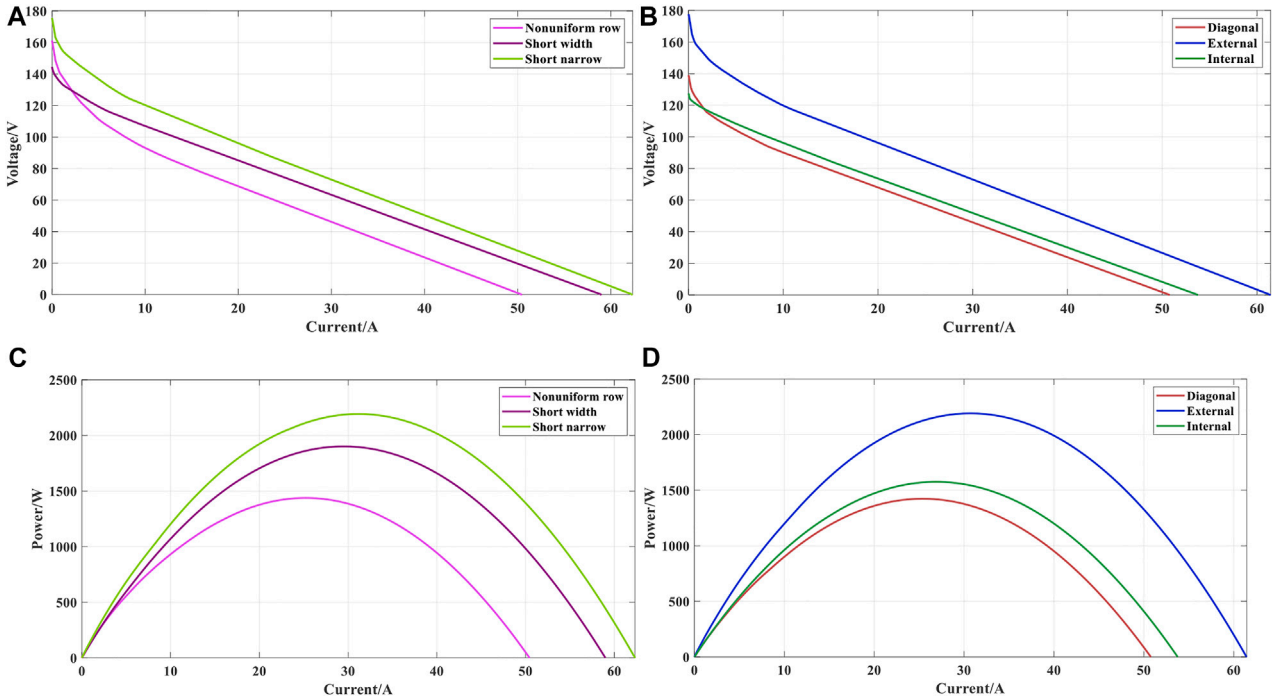

FIGURE 4 | Output characteristics curves of a 15 × 15 symmetric TEG array. **(A)** *V-I* curves from the a to c pattens, **(B)** *V-I* curves from the d to f pattens, **(C)** *P-I* curves from the a to c pattens, and **(D)** *P-I* curves from the d to f pattens.

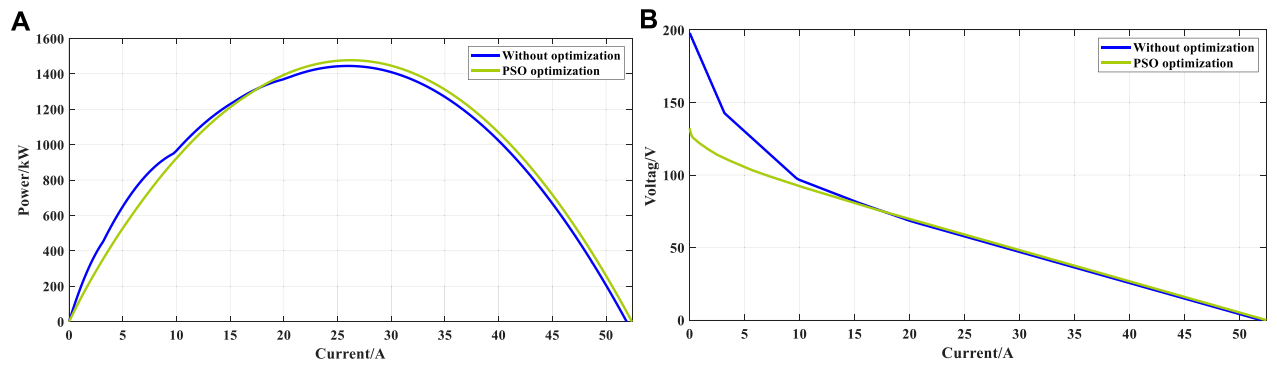

FIGURE 5 | The *V-I* and *P-I* curves with and without the optimization at pattern e **(A)** *V-I* curve at pattern e, **(B)** *P-I* curve at pattern e.

where $G_{mpp_{re}}$ is denoted GMPP found through reconfiguration of TEG array; $G_{mpp_{no}}$ stand for GMPP that can be found without reconfiguration of TEG array.

3 PARTICLE SWARM OPTIMIZATION ALGORITHM

3.1 Optimization Mechanism

PSO algorithm is a well established swarm intelligence optimization algorithm that exploits the information communication capabilities of a population to discover the optimal solution to a problem. PSO algorithm (Gavhane et al., 2017) is constructed from the concept of real-life bird foraging whereby each particle in the swarm is initialized with its corresponding fitness value, which corresponds to the solution to the problem. In addition, each particle memorizes the solution during each iteration (i.e., the individuals in the swarm retain their own best position for searching for food P_{best} as well as the best position obtained from the group G_{best}), which then begins to iterate. The

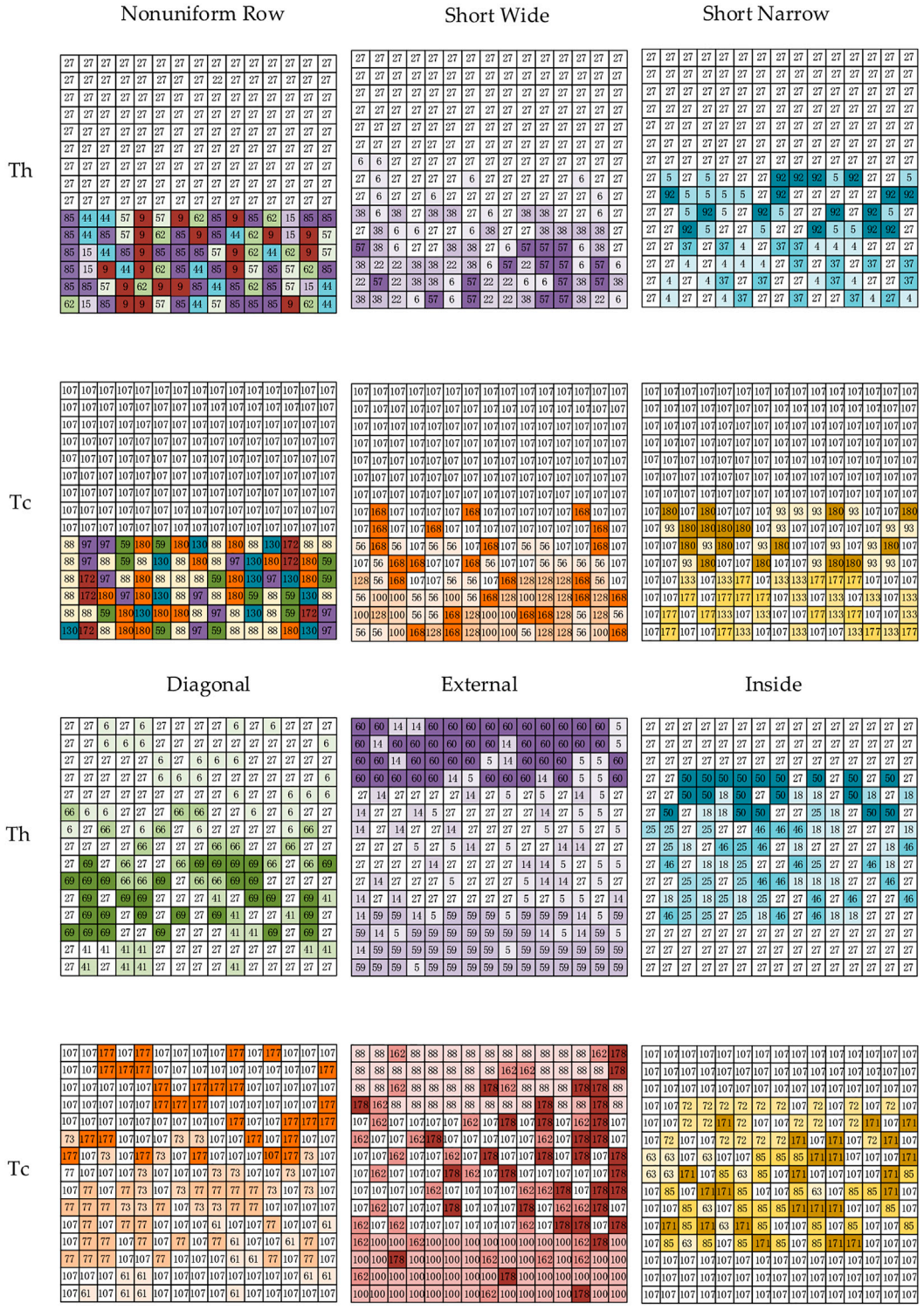

FIGURE 6 | Six HTD patterns in the 15 × 15 symmetric TEG array after reconfiguration.

iterative process is the process of each particle searching for the optimal solution, with the particles regulating their position and speed in accordance with the variation in fitness values to seek the optimal position, when all particles have converged to that position, that is the optimal solution to the problem. In particular, the velocity of the particle is denoted as V_i =

TABLE 2 | Output optimal power obtained by PSO algorithm under HTD conditions.

Serial Number	HTD Pattern	P_{un} (W)	PSO						
			P_{max} (W)	P_{min} (W)	P_{avg} (W)	STD (W)	P_{en1} (%)	P_{en2} (%)	P_{en3} (%)
A	Nonuniform row	1547.66	1569.53	1567.52	1568.36	0.391	1.413	1.283	1.338
B	Short width	1958.44	2006.39	2004.85	2005.58	0.367	2.448	2.369	2.407
C	Short narrow	2317.46	2342.26	2339.28	2340.22	0.674	1.070	0.942	0.982
D	Diagonal	1531.10	1572.26	1567.83	1568.64	0.861	2.688	2.399	2.452
E	External	2213.75	2309.05	2307.64	2308.24	0.338	4.305	4.242	4.269
F	Inside	1692.39	1735.17	1733.88	1734.47	0.282	2.528	2.452	2.486

$(V_{i1}, V_{i2}, \ldots V_{iD})$ together with the position is expressed as $X_i = (X_{i1}, X_{i2}, \ldots X_{iD})$.

Based on the principle of PSO algorithm, the mathematical model can be developed as follows: in a space of dimension D, a swarm of n particles searches for the optimal target, while the velocity and position of each particle are represented as

$$V_i(t+1) = \omega \cdot V_i(t) + c_1 \cdot r_1 \cdot (P_{\text{best}} - X_i(t)) + c_2 \cdot r_2 \cdot (G_{\text{best}} - X_i(t)) \tag{17}$$

$$X_i(t+1) = X_i(t) + V_i(t+1) \tag{18}$$

where V_i is denoted as the velocity of the ith particle in D dimensional space at time t+1; ω stands for the inertia weight of the particle, with a value range of 0–1; c_1 and c_2 are the learning factors used to adjust the trajectory and state of the particle; r_1 and r_2 represent the random factors, which are defined as random numbers between [0, 1]; *Pbest* is regarded as the optimal position of the individual in the particle memory; *Gbest* represents the optimal position obtained in the population; $X_i(t)$ is the position of the ith particle at the tth iteration.

In addition, the velocity and position of each particle are limited by boundary conditions in each iteration, as the particle may exceed the allowed search space and produce invalid solutions, while $V_{\max}$ is called velocity clamp as well as $X_{\max}$ and $X_{\min}$ mean position clamp.

3.2 Overall Optimization Procedure

For this reason, the overall implementation process of the reconfiguration design of TEG array based on PSO algorithm is depicted in **Table 1**.

4 CASE STUDIES

The array reconfiguration was carried out for six different HTD patterns (i.e., 1) Nonuniform row, 2) Short width, 3) Short narrow, 4) Diagonal, 5) External, 6) Inside) for a TEG array with a 15 × 15 symmetric topology. Furthermore, the results were derived from the optimization of PSO algorithm, which was compared with the results without reconfiguration. In addition, the maximum number of iterations K, the population size *Pop*, as well as the number of independent runs N_{run} were set at 30, 40, and 50, respectively. All the simulations were executed on MATLAB/Simulink 2019b via a personal computer with an IntelR CoreTM i5 CPU at 2.9 GHz and 16 GB of RAM.

Compared with the output power without reconfiguration, a comprehensive and holistic comparison of the reconfiguration performance of PSO algorithm in six HTD patterns is carried out. Furthermore, the six HTD distributions in the 15 × 15 symmetric TEG array are shown in **Figure 3**, where different colors indicate different temperatures and the number on each block represents the temperature of that module. **Figure 4** shows the output characteristics curves (i.e., *V-I* and *P-I* curves) of a 15 × 15 symmetric TEG array after reconfiguration. In particular, the maximum output power gained after PSO algorithm reconfiguration optimization is 4.305% higher than that gained without reconfiguration optimization under external temperature difference conditions, as illustrated in **Figure 5**. **Figure 6** depicts the high and low temperature distribution of the 15 × 15 symmetric TEG array for each UTD state after reconfiguration based on the PSO algorithm.

In addition, $P_{\max}$, $P_{\min}$, P_{avg}, and STD in **Table 2** are the maximum, minimum, average, and standard deviation of the output power of the PSO algorithm in 20 independent runs, while P_{en1}, P_{en2}, and P_{en3} in **Table 2** indicate the power enhancement values of the maximum output power, minimum output power, and average output power respectively, which are valuable for assessing the reliability and effectiveness of the TEG array using PSO algorithm. Under six UTD patterns (e.g., 1) Nonuniform row, 2) Short width, (c)Short narrow, 4) Diagonal, 5) External, 6) Inside), the power enhancement values of the maximum power are 1.413, 2.448, 1.070, 2.688, 4.305, 2.528% in turn. To sum up, PSO algorithm can be closer to GMPP through population search, which can remarkably enhance the reconfigured power of TEG array and effectively reduce power loss through a simple optimization mechanism and single search law.

5 CONCLUSION

This paper proposes a meta-heuristic optimization approach called PSO algorithm for TEG system reconfiguration under HTD conditions, which contains the following three contributions/novelties:

(1) This paper proposed a PSO to optimize TEG system reconfigures symmetric arrays, which has not been previously employed to achieve a fast and effective tracking of the MPPT under HTD conditions;
(2) This paper comprehensively considers the impact caused under HTD conditions and simulates the actual temperature distribution including six types of wasted heat. Besides, a design of electrical switching arrangement is performed for 15 × 15 symmetric TEG arrays so that it can easily deal with any HTD conditions;
(3) The switch matrix of electrical connection is controlled in real-time by PSO algorithm to realize the optimal reconfiguration of TEG system affected by HTD conditions, which effectively approximates GMPP;
(4) Compared with the common reconfiguration methods, PSO algorithm has good performance in global exploration and local exploitation, which can apparently reduce the probability of falling into LMPP.

PSO algorithm is also a model-free algorithm, which is highly independent of the specific mathematical model of the optimization problem. Hence, it has high application flexibility and can be employed for other optimization problems of energy conversion, such as MPPT of PV systems.

DATA AVAILABILITY STATEMENT

The original contributions presented in the study are included in the article/supplementary material, further inquiries can be directed to the corresponding author.

AUTHOR CONTRIBUTIONS

YZ: Conceptualization, Writing- Reviewing and Editing; EZ: Writing- Original draft preparation, Investigation; PN: Supervision.

FUNDING

This work is supported by Open Research Project of the State Key Laboratory of Industrial Control Technology, Zhejiang University, China (No. ICT 2022B66), Ningbo Natural Science Foundation (2019A610106), and Ningbo Science and Technology Major Project (20212ZDYF020044).

REFERENCES

Bijukumar, B., Raam, A. G. K., Ilango, G. S., and Nagamani, C. (2018). A Linear Extrapolation Based MPPT Algorithm for Thermoelectric Generators under Dynamically Varying Temperature Conditions. *IEEE Trans. Energy Convers.* 33 (4), 1641–1649. doi:10.1109/TEC.2018.2830796

Chakraborty, A., Saha, B. B., Koyama, S., and Ng, K. C. (2006). Thermodynamic Modelling of a Solid State Thermoelectric Cooling Device: Temperature-Entropy Analysis. *Int. J. Heat Mass Transf.* 49, 3547–3554. doi:10.1016/j.ijheatmasstransfer.2006.02.047

El-Dein, M. Z. S., Kazerani, M., and Salama, M. M. A. (2013). Optimal Photovoltaic Array Reconfiguration to Reduce Partial Shading Losses. *IEEE Trans. Sustain. Energy* 4 (1), 145–153. doi:10.1109/TSTE.2012.2208128

Fathy, A. (2020). Butterfly Optimization Algorithm Based Methodology for Enhancing the Shaded Photovoltaic Array Extracted Power via Reconfiguration Process. *Energy Convers. Manag.* 220, 113115. doi:10.1016/j.enconman.2020.113115

Fathy, A. (2018). Recent Meta-Heuristic Grasshopper Optimization Algorithm for Optimal Reconfiguration of Partially Shaded PV Array. *Sol. Energy* 171, 638–651. doi:10.1016/j.solener.2018.07.014

Fernández-Yáñez, P., Romero, V., Armas, O., and Cerretti, G. (2021). Thermal Management of Thermoelectric Generators for Waste Energy Recovery. *Appl. Therm. Eng.* 196, 117291. doi:10.1016/j.applthermaleng.2021.117291

Gavhane, P. S., Krishnamurthy, S., Dixit, R., Ram, J. P., and Rajasekar, N. (2017). EL-PSO Based MPPT for Solar PV under Partial Shaded Condition. *Energy Procedia* 117, 1047–1053. doi:10.1016/j.egypro.2017.05.227

Ge, M. H., Li, Z. H., Wang, Y. T., Zhao, Y., Zhu, Y., Wang, S., et al. (2021). Experimental Study on Thermoelectric Power Generation Based on Cryogenic Liquid Cold Energy. *Energy* 220, 119746. doi:10.1016/j.energy.2020.119746

Hasanien, H. M., Al-Durra, A., and Muyeen, S. M. (2016). "Gravitational Search Algorithm-Based PV Array Reconfiguration for Partial Shading Losses Reduction," in 5th IET International Conference on Renewable Power Generation (RPG), London, UK, 21-23 Sept. 2016, 703–708. doi:10.1049/cp.2016.0577

Jian, L., Zhen, Y., Li, H., Hu, S., Duan, Y., and Yan, J. (2021). Optimal Schemes and Benefits of Recovering Waste Heat from Data Center for District Heating by CO2 Transcritical Heat Pumps. *Energy Convers. Manag.* 245, 114591. doi:10.1016/j.enconman.2021.114591

Krishnan, S., Kinattingal, S. G., Simon, S. P., and Nayak, P. S. R. (2020). MPPT in PV Systems Using Ant Colony Optimisation with Dwindling Population. *IET Renew. Power Gener.* 14 (7), 1105–1112. doi:10.1049/iet-rpg.2019.0875

Lamzouri, F-E., Boufounas, E-M., Brahmi, A., and Amrani, A. E. (2020). Optimized TSMC Control Based MPPT for PV System under Variable Atmospheric Conditions Using PSO Algorithm. *Procedia Comput. Sci.* 170, 887–892. doi:10.1016/j.procs.2020.03.116

Li, X., WenHu, Y., and Jiang, L. (2018). A Novel Beta Parameter Based Fuzzy-Logic Controller for Photovoltaic MPPT Application. *Renew. Energy* 130, 416–427. doi:10.1016/j.renene.2018.06.071

Liu, Y. H., Chiu, Y. H., Huang, J. W., and Wang, S. C. (2016). A Novel Maximum Power Point Tracker for Thermoelectric Generation System. *Renew. Energy* 97, 306–318. doi:10.1016/j.renene.2016.05.001

Liu, J., Yao, W., Wen, J. Y., Fang, J., Jiang, L., He, H., et al. (2020). Impact of Power Grid Strength and PLL Parameters on Stability of Grid-Connected DFIG Wind Farm. *IEEE Trans. Sustain. Energy* 11 (1), 545–557. doi:10.1109/TSTE.2019.2897596

Luo, D., Wang, R., Yan, Y., Yu, W., and Zhou, W. (2021). Transient Numerical Modelling of a Thermoelectric Generator System Used for Automotive Exhaust Waste Heat Recovery. *Appl. Energy* 297, 117151. doi:10.1016/j.apenergy.2021.117151

Mamura, H., Üstünera, M. A., and AminBhuiyanb, L. R. (2022). Future Perspective and Current Situation of Maximum Power Point Tracking Methods in Thermoelectric Generators. *Sustain. Energy Technol. Assessments* 50, 101824. doi:10.1016/j.seta.2021.101824

Matthew, B., and Jae, D. P. (2015). Current-sensorless Power Estimation and MPPT Implementation for Thermoelectric Generators. *IEEE Trans. Industrial Electron.* 62 (9), 5539–5548. doi:10.1109/TIE.2015.2414393

Shahbaz, M., Raghutla, C., Chittedi, K. R., Jiao, Z., and Vo, X. V. (2020). The Effect of Renewable Energy Consumption on Economic Growth: Evidence from the Renewable Energy Country Attractive Index. *Energy* 207, 118162. doi:10.1016/j.energy.2020.118162

Sun, K., Yao, W., Fang, J. K., Ai, X., Wen, J., and Cheng, S. (2020). Impedance Modeling and Stability Analysis of Grid-Connected DFIG-Based Wind Farm with a VSC-HVDC. *IEEE J. Emerg. Sel. Top. Power Electron.* 8 (2), 1375–1390. doi:10.1109/JESTPE.2019.2901747

Yang, B., Wang, J. T., Zhang, X. S., Zhang, M., Shu, H., Li, S., et al. (2019). MPPT Design of Centralized Thermoelectric Generation System Using Adaptive Compass Search under Non-uniform Temperature Distribution Condition. *Energy Convers. Manag.* 199, 111991. doi:10.1016/j.enconman.2019.111991

Yang, B., Wang, J. B., Zhang, X. S., Yu, T., Yao, W., Shu, H., et al. (2020). Comprehensive Overview of Meta-Heuristic Algorithm Applications on PV Cell Parameter Identification. *Energy Convers. Manag.* 208, 112595. doi:10.1016/j.enconman.2020.112595

Yousri, D., Babu, T. S., Mirjalili, S., Rajasekar, N., and Elaziz, M. A. (2022). A Novel Objective Function with Artificial Ecosystem-Based Optimization for Relieving the Mismatching Power Loss of Large-Scale Photovoltaic Array. *Energy Convers. Manag.* 225, 113385. doi:10.1016/j.enconman.2020.113385

Zeddini, M. A., Pusca, R., Sakly, A., and Mimouni, M. F. (2016). PSO-Based MPPT Control of Wind-Driven Self-Excited Induction Generator for Pumping System. *Renew. Energy* 95, 162–177. doi:10.1016/j.renene.2016.04.008

Zhang, H. X., Lu, Z. X., Hu, W., and Tang, M. (2019). Coordinated Optimal Operation of Hydro-Wind-Solar Integrated Systems. *Appl. Energy* 242, 883–896. doi:10.1016/j.apenergy.2019.03.064

Zhang, R., Yang, B., and Chen, N. (2022). Arithmetic Optimization Algorithm Based MPPT Technique for Centralized TEG Systems under Different Temperature Gradients. *Energy Rep.* 8, 2424–2433. doi:10.1016/j.egyr.2022.01.185

Conflict of Interest: Authors EZ is employed by Ningbo Jianan Electronics Company Limited.

The remaining authors declare that the research was conducted in the absence of any commercial or financial relationships that could be construed as a potential conflict of interest.